AUV Turbulence Measurements in the LOCO Field Experiments

Louis Goodman
School for Marine Science and Technology (SMAST)
University of Massachusetts Dartmouth
706 South Rodney French Blvd
New Bedford, MA 02744
phone: (508) 910-6375 fax: (508) 910-6376 email: lgoodman@umassd.edu

Grant Number: N000140410254
http://www.smast.umassd.edu/Turbulence/

LONG-TERM GOAL

The long-term goal of this project is to quantify the role of turbulence and fine scale vertical shear and buoyancy on the formation, evolution, and breakdown of thin phytoplankton layers. Particular attention is given to understanding the relationship of the space and time statistics of the physical fields to that of the phytoplankton thin layers.

OBJECTIVES

(1) Quantify the horizontal and vertical structure of turbulence and identify the most probable mechanism of generation and maintenance. Particular attention will be given to the turbulent field arising from the internal wave train. Estimate the micro and fine scale parameters relating to thin layer studies: the turbulent dissipation rate, the buoyancy Reynolds number, the turbulent rms velocity, the turbulent eddy diffusivity, fine scale velocity shear, and fine scale stratification.

(2) Examine the role of turbulence on the evolution of the spatial structure of thin phytoplankton layers.

(3) Quantify the role of physical processes, such as turbulence mixing (diffusion), shear dispersion, and mean current advection on the temporal and spatial distribution and evolution of thin layers in the coastal ocean.

APPROACH

The observational approach is to use the Autonomous Underwater Vehicle, T-REMUS, shown in Fig. 1. T-REMUS is a custom designed REMUS 100 vehicle manufactured by Hydroid Inc., containing the Rockland Microstructure Measurement System (RMMS), an upward and downward looking 1.2 MHz ADCP, a FASTCAT Seabird CTD, and a WET Labs BB2F Combination Spectral Backscattering Meter/ Chlorophyll Fluormeter. In addition, the vehicle contains a variety of “hotel” sensors which measure pitch, roll, yaw, and other internal dynamical parameters.

This suite of sensors on T-REMUS allows quantification of the key dynamical and kinematical turbulent and finescale physical and biological processes (Goodman & Wang, 2008; Wang & Goodman, 2008). The turbulence measurements are made concomitantly with very high spatial

Report Documentation Page

Form Approved
OMB No. 0704-0188

1. REPORT DATE	2. REPORT TYPE	3. DATES COVERED
2008		**00-00-2008 to 00-00-2008**

4. TITLE AND SUBTITLE	5a. CONTRACT NUMBER
AUV Turbulence Measurements in the LOCO Field Experiments	5b. GRANT NUMBER
	5c. PROGRAM ELEMENT NUMBER
6. AUTHOR(S)	5d. PROJECT NUMBER
	5e. TASK NUMBER
	5f. WORK UNIT NUMBER
7. PERFORMING ORGANIZATION NAME(S) AND ADDRESS(ES) **University of Massachusetts Dartmouth,School for Marine Science and Technology (SMAST),706 South Rodney French Blvd,New Bedford,MA,02744**	8. PERFORMING ORGANIZATION REPORT NUMBER
9. SPONSORING/MONITORING AGENCY NAME(S) AND ADDRESS(ES)	10. SPONSOR/MONITOR'S ACRONYM(S)
	11. SPONSOR/MONITOR'S REPORT NUMBER(S)

12. DISTRIBUTION/AVAILABILITY STATEMENT
Approved for public release; distribution unlimited

13. SUPPLEMENTARY NOTES

14. ABSTRACT

15. SUBJECT TERMS

16. SECURITY CLASSIFICATION OF:			17. LIMITATION OF ABSTRACT	18. NUMBER OF PAGES	19a. NAME OF RESPONSIBLE PERSON
a. REPORT	b. ABSTRACT	c. THIS PAGE			
unclassified	**unclassified**	**unclassified**	**Same as Report (SAR)**	**9**	

resolution measurements of temperature, salinity, and depth. The BB2F sensor system measures chlorophyll fluorescence and optical backscattering at 470 nm and 700 nm wavelength. The turbulent and finescale parameters which can be estimated from the data collected by the T-REMUS include: the turbulent dissipation rate, the buoyancy Reynolds number, the turbulent velocity, finescale velocity shear, and finescale stratification. The thin phytoplankton layers are identified from chlorophyll a using the similar criteria as Dekshenieks et al. (2001).

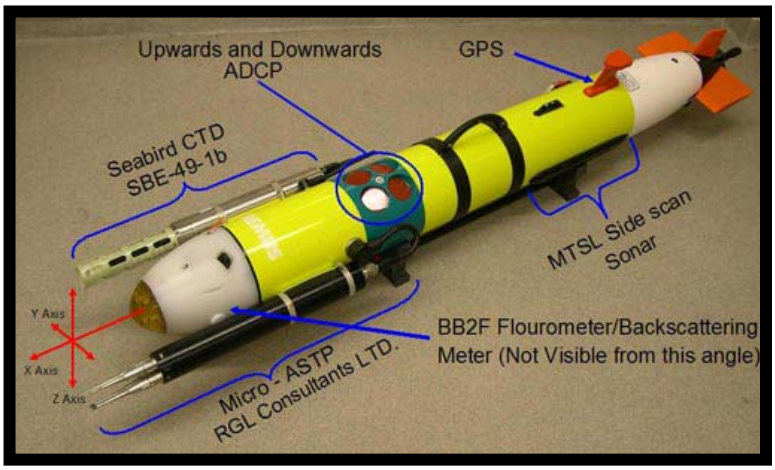

Figure 1, The SMAST T-REMUS Autonomous Underwater Vehicle. It is 2.0 m long, 20 cm diameter, and 63kg mass. Vehicle based sensors are indicated in the figure.

WORK COMPLETED

Two highly successful experiments were completed for LOCO 2005 and LOCO 2006 at the Monterey Bay site, centered near 36.93 N, 121.92W in the immediate vicinity of the fixed LOCO observatory stations deployed by Donaghay and Holliday, Figure 2b. During both LOCO 05 and LOCO 06 the T-REMUS performed flawlessly and had a remarkable 100 % data return. In both year experiments, the chlorophyll a and backscattering data showed significant thin layers. Data processing is completed for both LOCO 05 and 06 experiments with analysis now seriously underway. One manuscript "Turbulence Observations in the Northern Bight of Monterey Bay from a Small AUV" has been accepted for publication (July, 2008) by Journal of Marine Systems (JMS) and one "On the Evolution of the Spatial Structure of a Thin Phytoplankton Layer into a Turbulent Field" has just been accepted (September, 2008) by Marine Ecology Progress Series (MEPS). We are preparing our third manuscript "On the relationship of turbulence to thin phytoplankton layers" for submission to CSR for the LOCO special issues.

In LOCO 05, the T-REMUS performed a series of box of runs sides 2 to 3 km centered around the location of the principal LOCO moorings (fig 2b). The vehicle was operated with in a yoyo mode with a descent/ascent angle of 1 degree. This allowed thin layers to be resolved to 2 cm thickness. Eight such runs were performed, four of which were nighttime runs between 11:00 PM and 1: 00 AM, the time period of expected maximum occurrence and intensity of thin plankton layers.

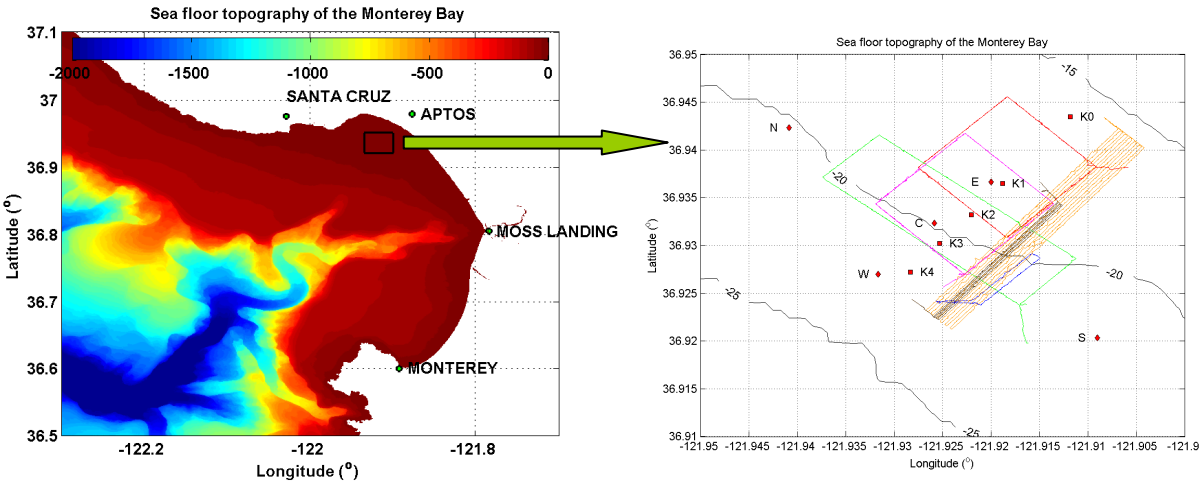

Figure 2, a) Map of the complex topography within and offshore of Monterey Bay. b) Detailed map showing the tracks of the T-REMUS AUV during LOCO. Also showed are the location of the fixed LOCO 2005 and 2006 stations.

In LOCO 06 sampling strategy for the T -REMUS was changed to increase horizontal resolution and to more closely parallel the fixed LOCO moorings, indicated by the salmon-colored lines in fig 2b. There were 12 continuous AUV tracks which ran parallel to the fixed LOCO observatory stations K0 to K4. These tracks were approximately perpendicular to isobath contours. Each track, 2.5 km in length, took 40 minutes and alternated between an outbound one and an inbound one. The AUV operated in a 5 degree yoyo mode with a ground speed of 1.2 m/s. AUV depth ranged from 1.0 m from the surface to 4.0 m above the bottom. Each track consisted of approximately 16 profiles with the horizontal distance between profiles being on average 150 m apart. Five 8-hour such data sets were collected during LOCO 06.

So far, our data analysis processes are focusing on the LOCO 06 data sets. We will now very briefly present some results germane to the issue of the spatial structure of turbulence and its role in the evolution of the spatial structure of a thin phytoplankton layer. For this analysis we examine in detail one particular, data set obtained from 19:00 PDT, 17 July 2006 to 03:00 PDT, 18 July 2006. Fine scale measurements of the horizontal and vertical spatial structure of the surrounding current, density field, Chlorophyll a and optical backscattering were obtained simultaneously. This sampling scenario not only allowed a detailed horizontal and vertical map of the turbulent field but also of the surrounding larger scale physical fields which drive the turbulence.

(1) The turbulence in the northern bight of Monterey Bay.

Figure 3 shows 12 contour plots of buoyancy Reynolds number, $\log_{10}(Re_b)$ as a function of across isobath range, r, and depth, z. Each contour was obtained on the 12 legs shown in Figure 2b. The origin of the abscissa, r = 0, is taken to be at the initial reference point at (36.942, -121.905). The experiment was conducted from 19:00 PDT 17 July 2006 to 03:00 PDT on the next day. The mean location of the profiles used to make these contour plots is indicated by a sequential number on the top of each contour panel. The reversal of profile ordering between panels is a result of the reversal of the heading of the AUV. The individual profiles are located on average 150 m apart in the across isobaths direction. The vertical black thick line is the across shore location of the fixed observational station

K1, shown in Fig. 2b, which is located 250 m northwest to the T-REMUS tracks. The black jagged line above the grey area indicates the seafloor bottom, which deepens from 16 m to 23 m going offshore. The starting time of the sampling for each contour plot as well as its leg number from 1 to 12 are shown in the grey area below the seafloor bottom. Each panel of the contour plots represents data sampled sequentially on average 40 minutes apart, or, using a mean current of 0.1 m s^{-1}, an upstream distance of 240 m apart. In each of these plots isotherms are spaced 0.2°C apart and shown as black lines. In addition to the buoyancy Reynolds number shown in Figure 3 we also have detailed spatial data on temperature, salinity, density, vector current, dissipation rate, turbulent velocity, chlorophyll-a, and optical scattering at 470 and 700 nm. The buoyancy Reynolds number is defined by

$$\mathrm{Re}_b = \frac{\varepsilon}{\nu N^2}$$

Where ε is the the dissipation rate of turbulent kinetic energy; $\nu = 10^{-6}$ $m^2 s^{-1}$ is the kinematic molecular viscosity; and N the buoyancy frequency. Re_b is a measure of the turbulent spatial dynamic range and is a better indicator of the strength of the turbulent field in a stratified fluid than ε. When $\mathrm{Re_b} > 200$, the turbulent field is fully developed and isotropic (Yamazaki & Osborn 1990). We will use the term "strong turbulence" to refer to that condition. When $\mathrm{Re_b} < 20$, stratification is sufficiently strong such that turbulence ceases to exist (Yamazaki & Osborn 1990). The panels in Fig. 3 show 3 regimes of strong turbulence with $\mathrm{Re_b} > 200$. These are: (1) a near surface regime associated with the warm water intrusion; (2) a bottom mixed layer regime; (3) a mid depth regime of strong vertical density (temperature) gradient. Note the very strong isolated patch of turbulence in what looks to be in the lee of an internal solitary wavelike feature in panel #5. This location of a turbulence patch relative to an internal solitary like wave is similar to that observed by Moum et al. (2003) off the Oregon coast.

Goodman & Wang (2008) have a detailed discussion on the most probable mechanisms for the turbulence generation in the three regimes. During the middle of the experiment at t = 21:30 PDT, a warm water surface intrusion was observed to evolve into a very strong frontal feature in which very strong turbulence occurred nearby. An upslope movement of the bottom mixed layer can be seen by following a near bottom isotherm, for example, the T = 11.2°C isotherm, initially located in panel #1 at the very lower left hand side of the panel. With time, it goes upslope for 900 m in 8 hours at the end of the experiment. Both the warm water surface intrusion and upslope movement of bottom mixed layer resulted in strong shear driven turbulence. The upslope transport of buoyancy in the most offshore location of the bottom mixed layer was approximately balanced by cross isopycnal turbulent buoyancy flux. Strong turbulence in the thermocline was noted towards the end of the experiment. Using the modal eKdV model of Grimshaw (2001), along with the observed values of internal wave displacement and local buoyancy frequency, indicated that internal wave induced shear and strain were not sufficiently strong to affect the mean local Richardson number. Moreover the largest internal wave induced effects in lowering the local Richardson number were predicted to occur at depths much shallower than that where the turbulence was observed. However, a theory was developed based on the approach of Moum et al. (2003) to examine the role of internal wave induced vertical strain gradient on inducing shear. It was shown that this effect of internal wave induced vertical strain was sufficiently strong to lower the local Richardson number below 1. At the end of the experiment strong turbulence was noted in the upper 10 m of the water column. Calculation of the effect of this turbulence on the internal wave train suggested a turbulent decay distance of 1.4 km. The AUV measurements have been unique in providing a detailed description of both the turbulent as well as larger scale flow field.

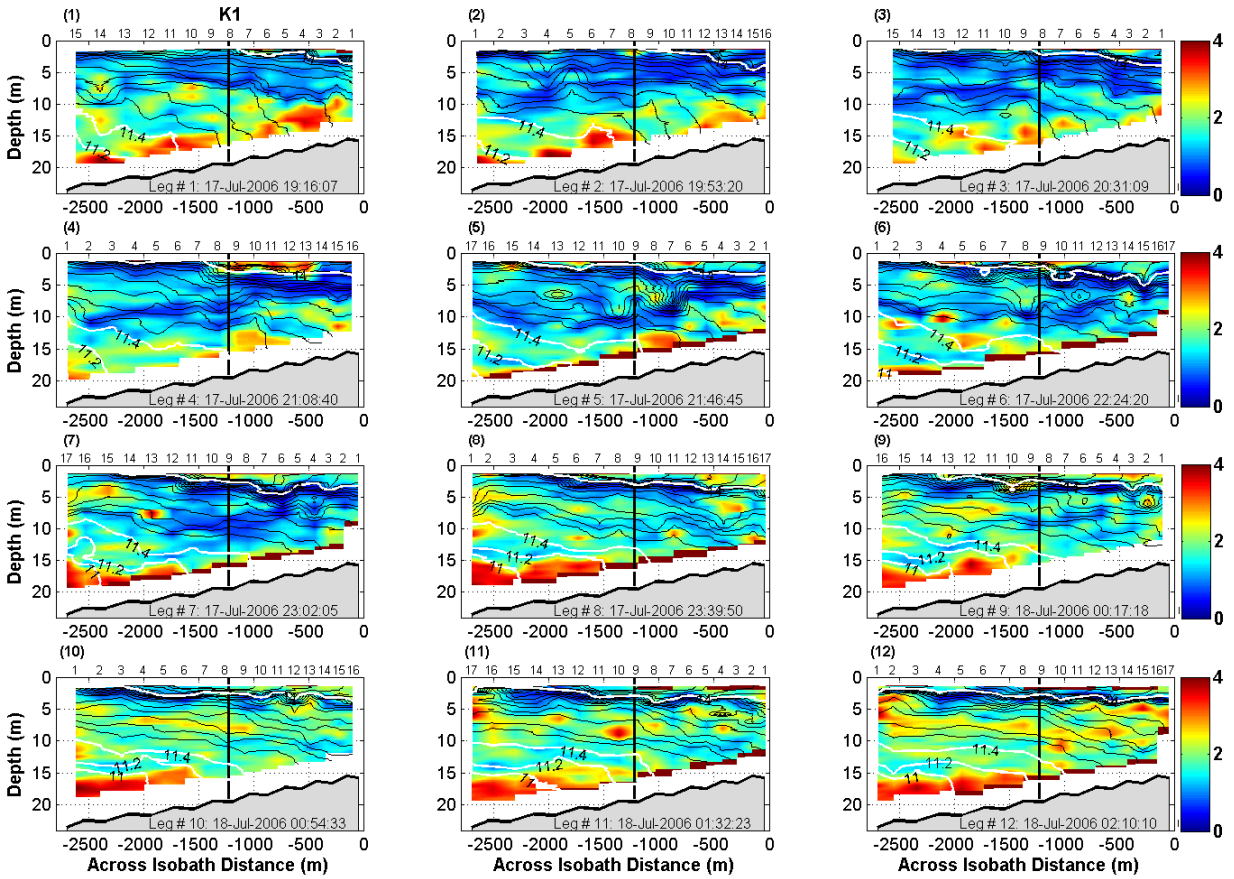

Fig. 3. Contour plots of buoyancy Reynolds number $\log_{10}(\mathrm{Re}_b)$ ***. Data were obtained from 07:00 PDT 17 July 2006 to 03:00 PDT 18 July 2006. Each contour was obtained on the 12 legs(salmon-colored lines) shown in Fig. 2b. Black contour lines show isotherms with 0.2 °C spacing. The numbers on the top of the contour map indicate profile number, located at their average location. The leg number and beginning time of each leg are showed at bottom of each figure. Isotherms of T = 11, 11.2, 11.4 and 14°C are emboldened in white. The across isobath location of the K1 thermistor chain is shown by the thick black line.***

(2) Evolution of the spatial structure of a thin phytoplankton layer into a turbulent field.

Fig. 4 shows chlorophyll *a* contour plots obtained from the T-REMUS BB2F fluorometer using the same data set of Fig. 3. The color bar scale to the right of each plot is in units of μg l^{-1}. As in the previous contour plot temperature isotherms are shown as black lines. Two isotherms are highlighted by white lines, one indicating T = 12.8°C showing a demarcation between the upper warm water layer and the mid water layer and one at T = 11.2°C which separates the mid water layer from that of the bottom mixed layer. Using our criteria of a thin layer, which must be three times greater than the background value, the T = 12.8°C separates two individual thin layers of chlorophyll *a*, which we term the upper and mid water thin layers, respectively. The upper thin layer occurs at the very beginning of the experiment at 19:00 PDT, 17 July 2006, well before sunset, which was at 20:30 PDT. It has a maximum chlorophyll *a* concentration of 60 μg l^{-1} (not shown in the figure) and is strongest near shore.

This upper thin layer weakens with time and eventually disappears by panel #7. Panel #4 shows what appears to be the beginning of the downward displacement of the upper thin layer chlorophyll *a* material inshore of K1. By panel #6 this results in its crossing of the T = 12.8°C isotherm into cooler, more dense water.

The mid water thin layer, which is located between isotherms T = 12.8 °C and T = 11.2 °C in Fig. 5, persists over the entire time period of the experiment, 8 hours. It has a horizontal across isobath scale of at least 1.5 km, which is probably an underestimate of its horizontal extent since it extends to the edge of the range of the T-REMUS measurements. Note the onshore stretching of the edge of this thin layer occurring along the isotherm T = 12.2°C and ranging between x = -1000 m in panel #1 to x = -500 m in panel #4. In panel #5 the isolated leading edge internal solitary wave which has propagated into the experimental site displaces this thin layer downward with the result that in panels #6 through #10 it appears that parts of the thin layer break up into several smaller pieces. The internal solitary wave of panel #5 also displaces downward the remnants of the upper thin layer with the result that in panels #6-12 the chlorophyll *a* concentration appears to undergo enhanced dispersion. The mid water thin layer does not penetrate through T = 11.2 °C isotherm which seems to act as a barrier to material migration.

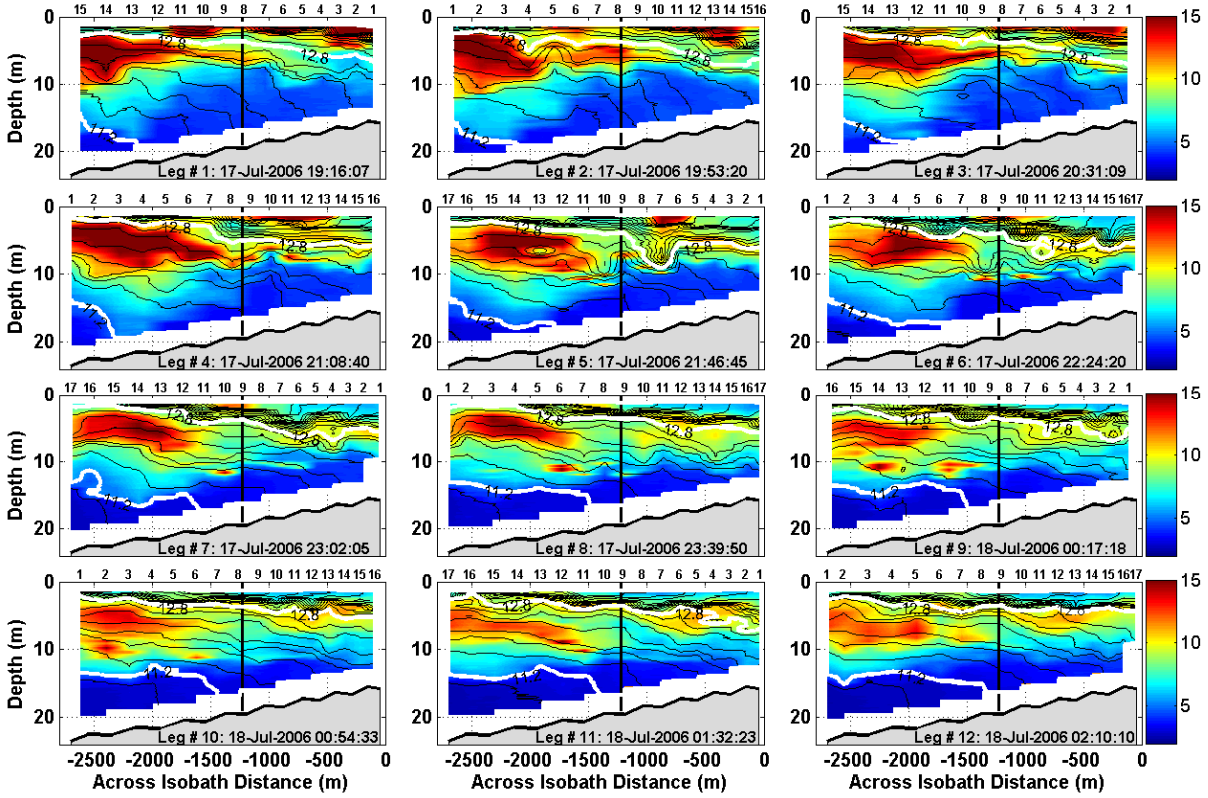

Fig. 4. Contour maps of the chlorophyll a (μg l^{-1}) as a function of across isobath distance and depth. Isotherms of temperature spaced 0.2°C apart are shown as black lines. Isotherms of T = 11.2 and 12.8 °C are emboldened in white.

Let us now examine in more detail the evolution of the mid depth chlorophyll *a* thin layer, which for the most part is located offshore of the K1 line. In Fig. 5, we show the temporal evolution of the depth

of center of mass of this thin layer taken relative to its initial depth, using the stretched vertical coordinate $\tilde{z}$. It shows initially constant values of the depth of the center of mass until 21:30 PDT. Changes in depth are noted during three periods: (i) from 21:30 PDT to 22:10 PDT; (ii) from 23:20 PDT to 01:20 PDT; and (iii) from 01:50 PDT to 02:30 PDT. The most significant change occurs during period (ii) when the center moves downward 2.1 meters. This corresponds to a downward speed of $w = 2.1m/(2\times 3600\,\text{sec}) \approx 290\ \mu\text{m s}^{-1}$. Period (i) is noted to occur at the time of the significant downward displacements associated with the isolated internal solitary wave (see Fig. 3, panel #5). Period (iii) was noted at the final time of the experiment when strong turbulence was observed in the thermocline throughout the experimental area.

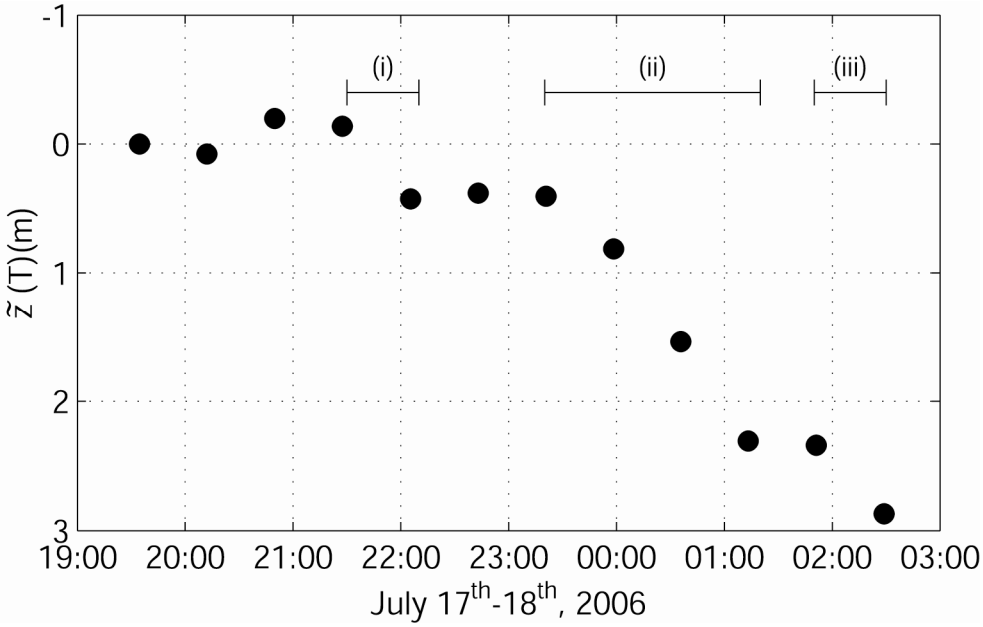

Fig.5. The change in depth of the center of mass of the mid depth chlorophyll a thin layer. A "stretched" vertical coordinate based on mean isotherm depth is used in the figure.

To examine in more detail the nature of the evolution of the thermocline based thin layer, we plot in Fig. 6 averaged vertical profiles of chlorophyll *a* in the thin layer, $\tilde{c}(\tilde{z},t)$. These profiles, $\tilde{c}(\tilde{z},t)$, are obtained by averaging over the most seaward four T-REMUS profiles of two consecutive legs. For the depth coordinate we use the stretched vertical coordinate $\tilde{z}$, discussed previously. In Fig. 6 the blue line is obtained from averages over legs 7, 8, the green line, over legs 9, 10 and the red line, over legs 11, 12. These profiles clearly show the deepening effect, which was observed in Fig. 5, for the thin layer mean vertical position. Between legs 7, 8 and legs 9, 10 there is a significant spreading of the profile, presumably due to the turbulent field also spreading, as indicated between panels 7, 8 and 9, 10 of Fig. 3. If we use the T-REMUS derived observed value of the eddy diffusivity of $\kappa_\rho \approx 5\times 10^{-5} m^2 s^{-1}$ during this time period (Wang & Goodman, 2008), over the time period change between the set of profiles of $\Delta t = 80$ minutes we would find that the rms change in the variance of these profiles given by $\Delta\sigma_z = \sqrt{2\kappa_\rho \Delta t} \approx 0.7m$, which is about the magnitude of the change in spread (about their respective maximum values) between the green and blue curves indicated in Fig 6. This supports the idea that the green curve evolves from the blue curve by a combination of sinking and turbulent diffusion. Again we note that this is a period of time of increasing turbulence in the mid layer.

Between legs 9, 10 and 11, 12 there is the opposite effect on the vertical structure of the chlorophyll *a* profile, namely a vertical contraction. This contraction is most probably the result of the collapse of the turbulent field by the surrounding stratification of the fluid. When the turbulent mixing results in eddies of the size of the buoyancy or Ozmidov scale, no further increase in the vertical extent of the turbulent field can occur (Tennekes and Lumley, 1972). A combination of some conversation of kinetic to potential energy as well as decay then results in the collapses of the turbulent field. This can be seen in some of the pioneering in situ dye studies of Woods (1968) showing the evolution of a turbulent as well as in turbulent wake collapse studies (Chernykh et al. 2005). Since the averaged terminal velocities of the phytoplankton in the thin layer estimated previously is much smaller than the turbulence velocity w' (Wang & Goodman, 2008), the thin layer material should follow fluid parcels as a Lagrangian tracer and collapse concurrently with the turbulent layer.

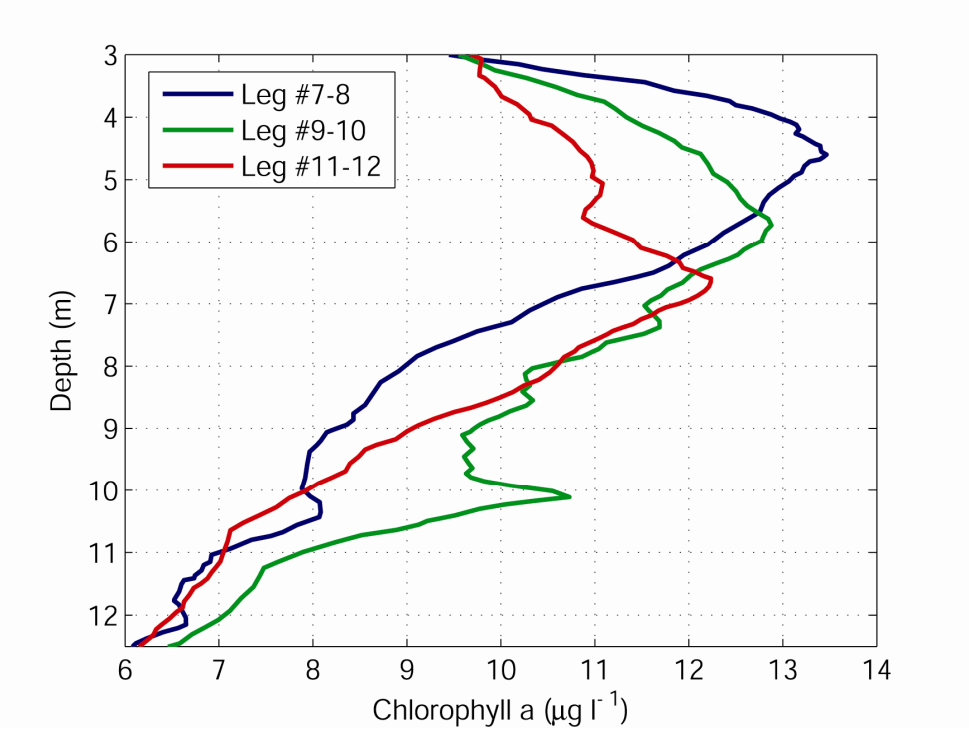

Fig. 6. Vertical profiles of the mid depth chlorophyll a thin layer, averaged over the most seaward four T-REMUS profiles of two consecutive legs in Fig 4 during the second half of experiment. The "stretched" vertical coordinate is used for depth.

IMPACT/APPLICATIONS

To date, there has been very few in situ studies on the direct effects of small-scale turbulence on thin layers. The platform T-REMUS provides a unique opportunity to quantify the spatial strcuture of the turbulence and fine scale fields and its relationship to thin layer formation evolutiona and breakdown. Our measurements show that the center of a thin layer deepened with time, crossed isotherms, and then settled into a strong turbulence layer. This result is in sharp contrast to previous conclusions that biological thin layers only occurred in regions of weak turbulence.

REFERENCES

Chernykh, GG, Fomina AV, Moshkin NP (2005) Passive scalar dynamics in turbulent wakes of bodies moving in a linearly stratified medium Russian Journal of Numerical Analysis and Mathematical Modelling. Vol 20 pp 403-423

Dekshenieks, M.M. Donaghay, P.L. etc. Temporal and Spatial Occurrence of Thin Phytoplankton Layers in Relation to Physical Processes. Marine Ecology Process Series, Vol. 223, pp 61-71, Nov. 2001.

Goodman, L. and Z. Wang, 2008, (in press), Turbulence observations in the northern bight of Monterey Bay from a small AUV, Journal Marine Systems.

Grimshaw, R., 2001. Internal solitary waves. Environmental stratified flows, Kluwer, Boston, Chapter 1. 1-28.

Moum, J.N., Farmer, D.M., Smyth, W.D., Armi, L. and Vagle, S., 2003. Structure and generation of turbulence at interfaces strained by internal solitary waves propagating shoreward over the continental shelf. J. Phys. Oceanogr ., 33, 2093-2112.

Tennekes H, Lumley JL (1972) A first course in turbulence, MIT ISBN 0262200198

Wang, Z. and L. Goodman, 2008, (accepted pending revision), On the evolution of the spatial structure of a thin phytoplankton layer into a turbulent field. Marine Ecology Progress Series.

Woods JD (1968) Wave-induced shear instability in the summer thermocline. J Fluid Mech, 32, 791-800

Yamazaki, H., and Osborn, T., 1990. Dissipation estimates for stratified turbulence. J. Geophys. Res., 95, 9739--9744, 1990.

PUBLICATIONS

Goodman, L. Levine, E.R., Lueck, R. On Measuring the terms of the Turbulent Kinetic Energy Budget from an AUV, Journal of Ocean and Atmospheric Technology, July 2006, pages 977-990.

Goodman, L. Robinson, A.R. On the Theory of Advective Effects on Biological Dynamics in the Sea, III: The Role of Turbulence in Biological Physical Interactions, Proc Royal Soc., Proceedings A 464 (2091), Mar 08, 2008.

Goodman, L. and Z. Wang, July 2008, (in press), Turbulence observations in the northern bight of Monterey Bay from a small AUV, Journal of Marine Systems.

Levine, E.R., **Goodman, L.,** O'Donnell, J., February 2008, (in press) Turbulence in coastal fronts near the mouth of Long Island Sound,invited J. Mar.Syst., Spec. Iss., Processes in Ocean Fronts.

Wang, Z. and **L. Goodman**, September 2008, (in press), On the evolution of the spatial structure of a thin phytoplankton layer into a turbulent field. Marine Ecology Progress Series.